

Minimum Row Weight and Polar Spectrum Based Puncture Polar Codes Construction Algorithm

Liu Daofu¹, and Guo Rui^{1*}

¹ School of Communication Engineering, Hangzhou Dianzi University, Hangzhou, China
[e-mail: guorui@hdu.edu.cn]

*Corresponding author: Guo Rui

*Received March 14, 2023; revised July 9, 2023; accepted July 31, 2023;
published August 31, 2023*

Abstract

In order to handle the problem that puncture patterns will change the position distribution of original information bits and frozen bits in polar codes, which affects performance of puncture polar codes further, a minimum row weight and polar spectrum based puncture polar codes construction algorithm (called PA-MRWP) is proposed in this paper. The algorithm calculates row weight of generator matrix and sorts the row weight in ascending order first. Next, the positions with the minimum row weight are selected as initial puncture positions. If the rows with the same row weight cannot all be punctured, polar spectrum based auxiliary puncture scheme is used. In sub-channels with the same row weight, rows corresponding to the polarized sub-channels with higher reliability are selected as puncture positions to construct puncture vector, and the reliability is calculated based on polar spectrum. It is actually a two-step selection strategy, the proposed minimum row weight puncture (MRWP) algorithm is used for primary selection and polar spectrum based auxiliary puncture is used for adjustment. Simulation results show that, compared with worst quality puncture (WQP) algorithm, the proposed PA-MRWP algorithm and Gaussian approximation-aided minimum row weight puncture (GA-MRWP) algorithm provide gains of about 0.46 dB and 0.29 dB at bit error rate (BER) of 10^{-4} , respectively when code length $N = 400$, code rate $R = 1/2$. In addition, the proposed puncture algorithms improve the BER performance significantly with respect to quasi-uniform puncture (QUP) algorithm.

Keywords: Generator matrix, Puncture, Polar spectrum, Polar codes, Row weight

1. Introduction

Polar codes [1] are a kind of channel coding with deterministic coding method designed by Arikan based on channel polarization theory, which have been theoretically proved to reach Shannon limit. After channel polarization, one part of the polarized sub-channels approach perfect channels with channel capacity 1, the other part of the polarized sub-channels approach pure noise channels with channel capacity 0. The key point of polar codes encoding is to estimate the reliability of polarized sub-channels. Researchers have proposed different sub-channels estimation methods such as Bhattacharyya parameter [2], density evolution (DE) [3], Gaussian approximation (GA) [4], and polarization weight (PW) [5].

The length of original polar codes is the power of two, i.e. $N = 2^n$, $n = 1, 2, \dots$. However, it is necessary to construct polar codes with arbitrary code length in actual communication. Therefore, puncture polar codes are designed to satisfy the actual needs. In [6], puncture was first proposed to construct polar codes, random puncture algorithm and stop-tree puncture algorithm were used to design rate-compatible puncture polar codes. QUP algorithm was proposed in [7], which made the puncture positions appear quasi-uniformly distribution by bit reversal sorting. However, QUP algorithm will lose the performance. Based on the generator matrix, a greedy algorithm was proposed in [8], which chosen the columns with weight 1 as puncture pattern, but the algorithm requires the receiver to know the value of the punctured bits. A low-complexity puncture algorithm was proposed in [9], and the puncture vector was obtained by bit-reversing the channel indexes. However, the algorithm comes at the cost of the performance loss. In [10], a hierarchical puncture algorithm was proposed to construct puncture polar codes by optimizing the information set. Considering the error probability of polarized sub-channels, WQP algorithm based on fixed information set was proposed in [11] to determine puncture pattern. In [12], an improved puncture algorithm was proposed based on bit-reversal puncture to support multi-coding rate system. In [13], the author exploited the density evolution to evaluate the error probability of punctured polar codes, and frozen bit positions are selected by genetic algorithm to construct a punctured polar code. A heuristic puncture algorithm of low rate polar codes was proposed in [14], which designed a kind of puncture pattern to avoid puncture on the fixed information set as much as possible. In [15], the author proposed a metric called reliability score which measures the reliability of LLR value at the information bit and punctured bits to maximize the minimum reliability score. In [16], the author proposed a novel method to construct puncture polar codes by enumerating specific Hamming distance, and executing combining and recursive decomposition operation.

PA-MRWP algorithm is proposed in this paper. The proposed algorithm considers the structure of polar codes, and optimizes the puncture pattern by combining row weight of generator matrix and the reliability of polarized sub-channels. The algorithm calculated row weight and sorts the row weight in ascending order first. Then, the positions with smaller row weight are chosen as initial puncture positions. If the rows with the same row weight cannot all be punctured, polar spectrum based auxiliary puncture scheme is used. Based on the initial puncture positions, rows corresponding to the polarized sub-channels with higher reliability is selected as puncture positions to construct puncture vector. Simulation results show that, proposed algorithms can optimize puncture pattern and improve performance of puncture polar codes. Moreover, the calculation of both the row weight and the polar spectrum proposed in this paper is independent of the real-time signal-to-noise ratio and can be carried out offline.

The rest of this paper is as follows. In Section 2, basic principles of polar codes and polar spectrum are presented. The proposed puncture algorithms are described in Section 3. Simulation results of the proposed puncture algorithms are presented in Section 4. Section 5 summarizes the paper.

2. Preliminaries

2.1. Basic Principle of Polar Coding

Assume that length of polar code is $N = 2^n, n \geq 0, u_1^N \rightarrow x_1^N$ denotes the mapping of the original bit sequence u_1^N to the encoded bit sequence x_1^N . The encoding process is

$$x_1^N = u_1^N \mathbf{G}_N \tag{1}$$

$$\mathbf{G}_N = \mathbf{B}_N \mathbf{F}^{\otimes n} \tag{2}$$

Where \mathbf{G}_N is generator matrix, \mathbf{B}_N is the bit-reversal permutation matrix. And $\mathbf{F}^{\otimes n}$ is a matrix of $N \times N$, denotes n th Kronecker product of matrix $\mathbf{F} = \begin{bmatrix} 1 & 0 \\ 1 & 1 \end{bmatrix}$, the calculation formula is

$$\mathbf{F}_N = \mathbf{F}^{\otimes n} = \mathbf{F} \otimes \mathbf{F}^{\otimes(n-1)} \tag{3}$$

2.2. Polar Spectrum

Based on the encoding structure of polar codes, polar spectrum [17] uses matrix \mathbf{F}_N to estimate the reliability of polarized sub-channels. N polarized sub-channels can be obtained after channel polarization. It is defined that the first $i - 1$ bits of the bit vector \mathbf{c} corresponding to the i th polarized sub-channel are fixed to 0, and the remaining positions are set to 0 or 1. The number of bit vector of the i th polarized sub-channel is 2^{N-i+1} , the number of codeword vector is also 2^{N-i+1} . The codeword vector can be expressed as

$$\mathbf{y} = \mathbf{c} \mathbf{F}_N \tag{4}$$

The Hamming weight distribution of the codeword vector is expressed as the weight enumerator $S_N^{(i)}(d)$, where i is the polarized sub-channel index, and d is the Hamming weight. For example, when code length is 4, the Hamming weight of polarized sub-channel $i = 3$ is shown in **Table 1**.

Table 1. Hamming weight

Bit vector \mathbf{c}	Codeword vector \mathbf{y}	Hamming weight d
[0 0 0 0]	[0 0 0 0]	0
[0 0 0 1]	[1 1 1 1]	4
[0 0 1 0]	[1 0 1 0]	2
[0 0 1 1]	[0 1 0 1]	2

According to (4), the weight distribution of all polarized sub-channels can be obtained. Polar spectrum $A_N^{(i)}(d)$ is denoted as

$$\begin{cases} A_N^{(i)}(0) = 0 & , i = 1, 2, \dots, N \\ A_N^{(i)}(d) = S_N^{(i)}(d) - S_N^{(i+1)}(d), & i = 1, 2, \dots, N-1 \\ A_N^{(i)}(d) = S_N^{(i)}(d) & , i = N \end{cases} \quad (5)$$

Where d is the Hamming weight, and i is polarized sub-channel index.

The calculation of polar spectrum is usually complex. In [17], the dual codes of linear block codes and the MacWilliams identities are used to simplify solving process. The method of recursively solving the polar spectrum is as follows:

1) When polar spectrum of polar code with code length N is known. The formula for calculating the polar spectrum corresponding to the lower half of polar code with code length $2N$ is written as

$$\begin{cases} A_{2N}^{(l)}(p) = A_N^{(i)}(d), p = 2d \\ A_{2N}^{(l)}(p) = 0 & , p < 2N \text{ and } p = 2k-1 \end{cases} \quad (6)$$

Where $l = N + i, i = 1, 2, \dots, N$, p is the Hamming weight, k is positive integer.

2) The weight distribution of the lower half of polar code with code length $2N$ is written as

$$\begin{cases} S_{2N}^{(l)}(p) = S_{2N}^{(l+1)}(p) + A_{2N}^{(l)}(p), p = 0, 1, \dots, 2N \text{ and } l \neq 2N \\ S_{2N}^{(l)}(p) = A_{2N}^{(l)}(p) & , p = 1, 2, \dots, 2N \text{ and } l = 2N \\ S_{2N}^{(l)}(p) = 1 & , p = 0 \text{ and } l = 2N \end{cases} \quad (7)$$

3) The weight distribution of the upper half with channel index 1 to N is calculated by the MacWilliams identities. Then the weight enumerator with code length $2N$ is obtained. Finally, (5) is used again to calculate polar spectrum of the upper half of polar code with code length $2N$.

According to polar spectrum, the simplified union-Bhattacharyya weight (SUBW) can be used to measure the reliability of polarized sub-channels. In AWGN channels, the SUBW is expressed as

$$SUBW_N^{(i)} = \ln \left[A_N^{(i)} \left(d_{\min}^{(i)} \right) \right] - d_{\min}^{(i)} \frac{E_s}{N_0} \quad (8)$$

Where signal-to-noise (SNR) is independent of the original channel parameters, and can be represented by a constant α . In practical applications, the optimal value can be selected according to the actual application scenario.

Polar codes usually rely on the information of original channel. The reliability of polarized sub-channels is estimated by recursive formula. If the parameters of channel change, the estimation result of reliability will be affected. However, the polar spectrum does not depend on the parameters of channel, and can measure the reliability of polarized sub-channels more intuitively and explicitly.

3. Puncture Polar Codes Construction Algorithm

3.1. The Principle of Puncture

The essence of puncture is to delete part of encoded bits of the polar codes, so as to achieve the purpose of dynamically changing the code length and code rate. According to the

puncture vector, some bits of the original encoded bits is deleted. The puncture vector can be expressed as

$$\mathbf{p} = (p_1, p_2, \dots, p_N) \quad (9)$$

Where $p_i \in \{0, 1\}$, $i = 1, 2, \dots, N$. $p_i = 0$ denotes the bit at this position will be punctured. $p_i = 1$ denotes the coded bit is reserved.

During communication process, the encoded bits at the puncture positions are not transmitted through the actual physical channel. However, the channel polarization result will be affected by the puncture algorithm, thereby affecting reliability of the sub-channels. There are two kinds of puncture polar codes construction method: the method based on reconstruction and the method based on non-reconstruction. For the puncture polar codes based on the reconstruction, the reliability of polarized sub-channels needs to be recalculated after puncture according to the puncture pattern, and information bit set is selected accordingly. Reconstruction increases the complexity of the algorithm. For the puncture polar codes based on non-reconstructed method, the reliability of polarized sub-channels does not need to be recalculated after puncture, and the information bit set is determined according to the reliability of original polarized sub-channels and puncture pattern. During decoding, the Log likelihood ratio value corresponding to deleted encoded bits will be reset to 0. Since the puncture operation will change the original position of information bits and frozen bits set in polar codes, performance can be improved by optimizing the puncture pattern to satisfy the transmission requirements of the actual system.

3.2. Proposed MRWP Algorithm

The structure of polar codes is related to the generator matrix. It can be seen from (1) that each row of the generator matrix has an element involved in the calculation of each encoded bit. Theoretically, the optimal puncture pattern of puncture polar codes can be constructed by optimization of distance spectrum or minimum Hamming distance. But distance spectrum is difficult to be calculated. The minimum Hamming distance can be represented by the minimum row weight of generator matrix to evaluate performance of puncture algorithm [7]. In this paper, we choose the rows with smaller row weight as the puncture positions. In [Table 2](#), the distribution of row weight in the generator matrix obeys Pascal's triangle law.

Table 2. Row weight distribution of generator matrix

Code length	Row weight						
	1	2	4	8	16	32	64
8	1	3	3	1			
16	1	4	6	4	1		
32	1	5	10	10	5	1	
64	1	6	15	20	15	6	1

In order to design the puncture pattern, the MRWP algorithm based on the generator matrix is proposed. Since the distribution of rows with the same row weights in the generator matrix is scattered, the distribution of puncture positions obtained by row weight is close to

quasi-uniform. The specific steps for constructing the puncture polar codes based on the non-reconstructed are shown in [Table 3](#).

Table 3. Puncture polar codes construction based on MRWP algorithm

Input: Original code length N , puncture number N_p , information bits K , and code length of puncture polar codes M
Output: Puncture vector \mathbf{P}
1) Calculate the row weight.
2) According to the ascending order of row weight, encoded bits corresponding to the rows with the smaller row weight are selected as the puncture positions.
3) If the rows with the same row weight cannot all be punctured, select one of the rows to puncture randomly.
4) Preset N_p polarized sub-channels corresponding to the puncture vector $p_i = 0$ as frozen bits.
5) According to the original polarized sub-channels reliability, select K channels with the highest reliability from the remaining polarized sub-channels as information set, and the rest are selected as frozen set.
6) Delete the coded bits in position $p_i = 0$. After puncture, puncture polar codes with code rate K/M are obtained.

3.3. Puncture Polar Codes Construction Algorithm Based on Minimum Row Weight and Polar Spectrum

3.3.1 The Auxiliary Puncture Scheme

The proposed MRWP algorithm preferentially selects the positions with smaller row weight to generate puncture pattern. When the rows of the same row weight cannot all be punctured, the proposed MRWP algorithm randomly selects the puncture positions among the same row with the same weight, which will lead to unstable performance. To further improve the performance, auxiliary scheme is used to aid selecting puncture positions.

Suppose that code length is N and number of puncture bits is N_p . When N_p satisfies

$$N_p^{(w_0)} + N_p^{(w_1)} + \dots + N_p^{(w_{n-1})} < N_p < N_p^{(w_0)} + N_p^{(w_1)} + \dots + N_p^{(w_n)}, \quad n = 1, 2, 3, \dots, \log_2(N) \quad (10)$$

the auxiliary puncture scheme is used. Where $\mathbf{w}_0^n = (w_0, w_1, w_2, \dots, w_n) = (1, 2, 4, \dots, 2^n)$ denotes row weight, $N_p^{(w_n)}$ denotes number of the same row weight.

When rows with the same row weight cannot be punctured at the same time, three auxiliary puncture schemes can be proposed.

Scheme 1: The positions corresponding to polarized sub-channels with higher reliability is selected for puncture.

Scheme 2: Select the positions corresponding to polarized sub-channels with lower reliability for puncture.

Scheme 3: QUP algorithm is used to assist the selection of puncture positions.

Suppose that code length is N , the error probability of sub-channels can be expressed as $\mathbf{p}_e = \{p_e^{(1)}, p_e^{(2)}, p_e^{(3)}, \dots, p_e^{(N)}\}$. The error probability of sub-channels and normalized row weight distribution of the generator matrix are shown in [Fig. 1](#). The blue dot is the sub-channels reliability distribution, and the green dot is the normalized row weight

distribution. It can be seen from the figure that the positions with low reliability and low row weight overlap in a large proportion, especially in the areas with low reliability. As number of puncture bits increases, when the rows with the same weight cannot all be punctured, if the sub-channels with low reliability is selected for puncture, these positions are most likely to be together with the punctured low row weight positions. In this case, it is similar to the sequential puncture, which reduces performance of the polar codes. However, if the sub-channels with higher reliability is selected for puncture, puncture positions are scattered which avoids the occurrence of sequential puncture. In other words, the sub-channels with higher reliability are selected for puncture when the rows with the same weight cannot all be punctured, which reduces the density of puncture positions obtained by previous accumulation.

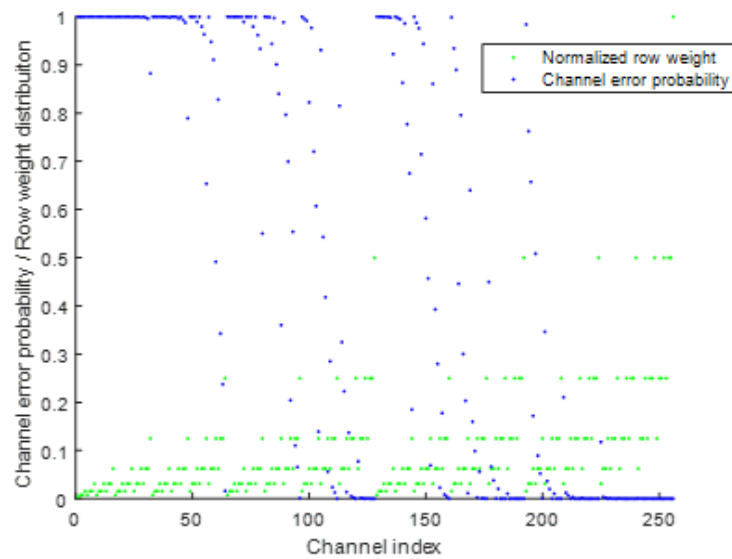


Fig. 1. Channel error probability distribution and row weight distribution

For code length is $N = 128$, sub-channel indexes of partial row weight are shown in **Table 4**. When the number of puncture bits is 48, the channels of the rows with weight 1, 2, and 4 are all selected as puncture positions. In addition, we need to use the auxiliary puncture scheme to select the puncture positions in the rows with weight 8. In **Table 5**, the final puncture positions determined by three different auxiliary puncture schemes are listed respectively. Among them, the bold indexes are selected for puncture. The channel index dispersion of the three schemes is calculated by variance, which are $s_1 = 1112.83$, $s_2 = 566.32$, and $s_3 = 778.62$ respectively. It can be seen that the final puncture positions selected by the scheme 1 are more dispersed than those of the scheme 2 and the scheme 3.

Table 4. Channel indexes corresponding to partial row weight

Row weight	Channel index
1	1
2	2,3,5,9,17,33,65
4	4,6,7,10,11,13,18,19,21,25,34,35,37,41,49,66,67,69,73,81,97
8	8,12,14,15,20,22,23,26,27,29,36,38,39,42,43,45,50,51,53,57,68,70,71,74,75,77,82,83,85,89,98,99,101,105,113

Table 5. Puncture positions under different auxiliary puncture schemes

Scheme	Puncture positions index	Dispersion
Scheme 1	1,2,3,4,5,6,7,9,10,11,13,17,18,19,21,25,33,34,35,37,41, 45,49,50,51,53,57,65,66,67,69,70,71,73,74,75,77,81,82,83,85,89,97,98,99,101,105,113	$s_1 = 1112.8$
Scheme 2	1,2,3,4,5,6,7,8,9,10,11, 12,13,14,15 ,17,18,19, 20,21,22,23,25,26,27,29 ,33,34,35, 36,37,38,39 ,41, 42,43,45,49,50,65,66,67,68,69,70,73,81,97	$s_2 = 566.3$
Scheme 3	1,2,3,4,5,6,7,8,9,10,11, 12,13,14 ,17,18,19, 20,21,23,25,27,29 ,33,34,35, 36,37,39,41,43,49,50,51,53,65,66,67,68,69,71,73,75,81,82,85,97,98	$s_3 = 778.6$

3.3.2 Proposed PA-MRWP Algorithm

The PA-MRWP algorithm is presented in this section, which chooses scheme 1 as the auxiliary puncture scheme. It is actually a two-step selection strategy. MRWP algorithm is used for primary selection and auxiliary puncture is used for fine adjustment. Firstly, the proposed algorithm computes the Hamming weight of each row in the constructed generator matrix. Then puncture positions are selected for puncture in ascending order based on row weight. If the rows with the same row weight cannot be fully punctured, we use the polar spectrum to evaluate the reliability of polarized sub-channels. Finally, auxiliary puncture scheme is taken, and the rows corresponding to polarized sub-channels with higher reliability are preferentially selected as puncture positions, which can avoid dense puncture affecting the performance.

Only when polarized sub-channels corresponding to row weight cannot all be used as puncture positions, the polar spectrum auxiliary puncture method is used to select the channels with higher reliability among these sub-channels. Other channel estimation algorithms, such as GA can be used to estimate the channel reliability. The detailed process of PA-MRWP algorithm is described in **Table 6**.

Table 6. Proposed PA-MRWP Algorithm

Input: Original code length $N = 2^n$, puncture number N_p , row weight r , <i>SUBW</i> value
Output: Puncture vector \mathcal{P}
<pre> 1 for $i = 1$ to n do 2 $\mathbf{G}_N \leftarrow \text{kron}(\mathbf{F})$ Generator matrix 3 end for 4 $r_i \leftarrow \text{sum}(\mathbf{G}_N)$ Row weight 5 for $ii = 1$ to N do 6 $B(ii) \leftarrow \text{length}(r_i = ii)$ Statistical row weight distribution 7 $A \leftarrow \text{sum}(B(ii))$ Number of row weight is superimposed 8 if $A \leq N_p$ then 9 $p_1 = 0$ Puncture 10 else 11 break 12 end if 13 end for 14 if The number of puncture is less than N_p then</pre>

```

15      $p_2 = 0 \leftarrow \text{sort}(SUBW)$  Puncture
16     return  $\mathbf{p} \leftarrow (p_1, p_2)$ 
17 else
18     return  $\mathbf{p} \leftarrow p_1$ 
19 end if

```

In **Table 6**, the korn function in row 2 is used to get the generator matrix. The SUM function in row 4 is used to calculate row weight. The SORT function in row 15 represents that the quality of polarized sub-channels estimated by using the polar spectrum.

For example, original code length is $N = 8$. After puncture, code length is $M = 5$. **Fig. 2** shows the specific generator matrix with row weight $\mathbf{w} = (1, 2, 2, 4, 2, 4, 4, 8)$. The encoded bit corresponding to row the h_1 with row weight of 1 is selected. At the same time, the encoded bit x_1 is deleted. It is obvious that the partial puncture vector obtained is $\mathbf{p}_1 = (01111111)$. For the row with row weight of 2, there are multiple rows that satisfy the puncture conditions. However, they cannot all be deleted. So, we preferentially select the row corresponding to the polarized sub-channel with higher reliability as puncture positions. The corresponding *SUBW* values of the candidate rows h_2, h_3, h_5 are $-3.2274, -3.9206, -4.6137$, respectively. As shown in **Fig. 3**, h_3 and h_5 with greater reliability of polarized sub-channels are chosen as the puncture positions. The final puncture vector is $\mathbf{p} = (01010111)$. During polar encoding process, the polarized sub-channels with channel indexes of 1, 3, and 5 are preset as frozen bits.

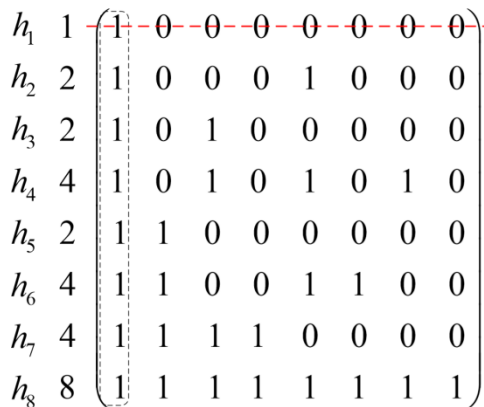


Fig. 2. Schematic diagram of first puncture

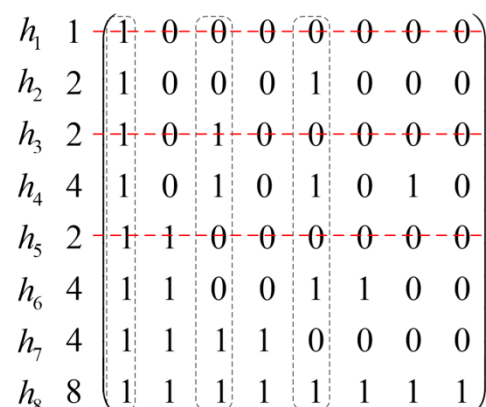


Fig. 3. Schematic diagram of auxiliary scheme puncture

4. Simulation Results

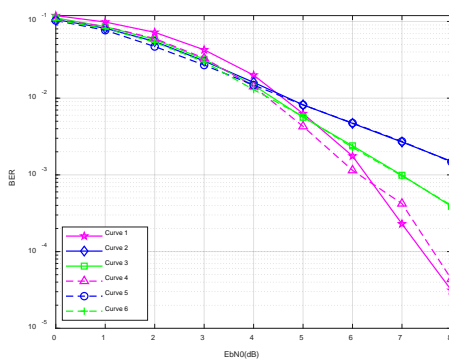
Simulation results of proposed PA-MRWP puncture polar codes construction algorithm are shown in this section. In addition, the WQP algorithm and QUP algorithm is also given for comparison. In the WQP algorithm and QUP algorithm, we can either use Gaussian Approximation (GA) or polar spectrum (PS) to measure the reliability of sub-channels. When the reliability of sub-channels is estimated by polar spectrum, the SNR is set to constant $\alpha = 3$ dB as shown in (8). Corresponding to the PA-MRWP algorithm, when GA is

also used to measure the reliability of sub-channels, this algorithm is called GA-MRWP algorithm. In the experiment, the polar codes are modulated by BPSK in the AWGN channels. In the simulation process, successive cancellation (SC) decoding algorithm [2] and CRC-aided SCL(CA-SCL) decoding algorithm [18] is adopted.

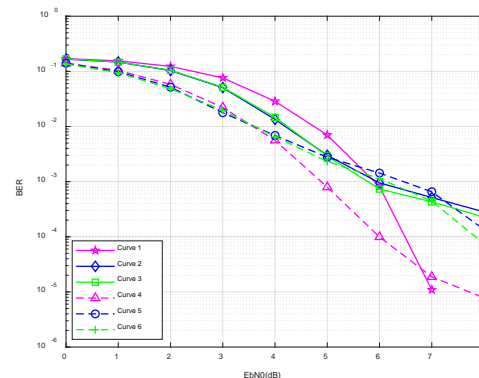
Fig. 4 shows the BER performance of proposed different auxiliary puncture schemes in SC decoding. The length of mother code is 128 and 256 respectively. After puncture, the code rate is 1/2. For comparison, PS and GA are used as the channel reliability estimation methods. For the convenience of description, the abbreviations are shown in **Table 7**. In **Fig. 4(a)** and **Fig. 4(b)**, the curve 1 can get better performance than the curve 2 and 3 obviously, and the curve 4 can get better performance than the curve 5 and 6. To sum up, scheme 1 can achieve better performance.

Table 7. Abbreviations for different methods

Abbreviation	Description
Curve 1	PS + scheme 1
Curve 2	PS + scheme 2
Curve 3	PS + scheme 3
Curve 4	GA + scheme 1
Curve 5	GA + scheme 2
Curve 6	GA + scheme 3



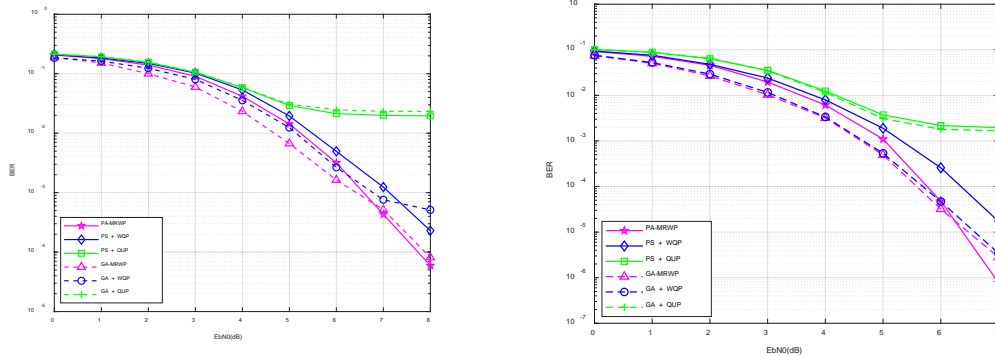
(a) (128, 80, 40) Puncture polar codes



(b) (256, 192, 96) Puncture polar codes

Fig. 4. Performance comparison of proposed different auxiliary puncture schemes

The BER performance of the proposed puncture algorithms in SC decoding is shown in **Fig. 5**. The WQP algorithm and QUP algorithm is also given for comparison. At the same time, in the different puncture algorithms, PS and GA are used as the channel reliability estimation methods. The length of mother code is 128, the length of puncture polar code is 96, and code rate of puncture polar code is 2/3. In **Fig. 5(a)**, the proposed PA-MRWP algorithm can get about 0.54 dB gain than the WQP algorithm at BER of 10^{-3} , and proposed GA-MRWP algorithm can get about 0.35 dB gain than WQP algorithm at BER of 10^{-3} . In **Fig. 5(b)**, the original code length is 256, the length of puncture polar code is 180, and code rate of puncture polar code is 1/3. Compared with WQP algorithm, the proposed PA-MRWP algorithm and GA-MRWP algorithm obtain gains of about 0.58 dB and 0.10 dB respectively at BER of 10^{-4} . In **Fig. 5(a)** and **Fig. 5(b)**, the proposed PA-MRWP algorithm and GA-MRWP algorithm significantly outperform the QUP algorithm.

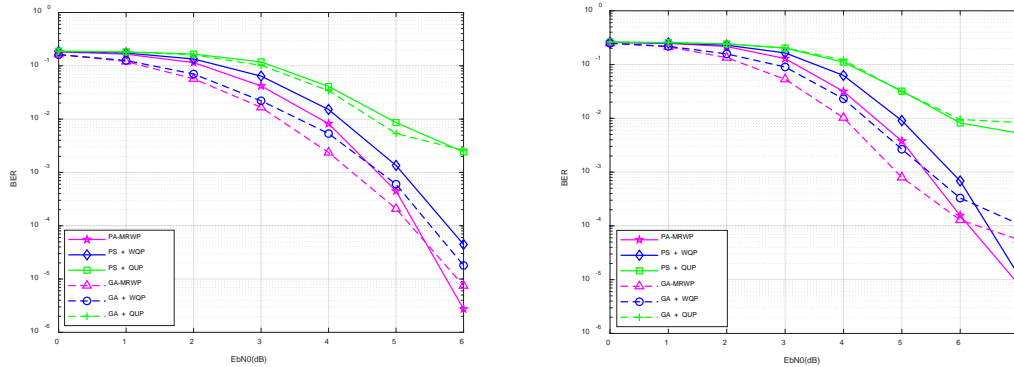


(a) (128, 96, 64) Puncture polar codes

(b) (256, 180, 60) Puncture polar codes

Fig. 5. Performance comparison of puncture algorithms for different code length

In Fig. 6, we show the BER of different puncture algorithms with the original code length 512 in SC decoding. After puncture, the length is 400, and code rate of puncture polar code is 1/2. As shown in Fig. 6(a), the proposed PA-MRWP algorithm and GA-MRWP algorithm can get 0.46 dB and 0.29 dB gain respectively at BER of 10⁻⁴ as compared with WQP algorithm. In Fig. 6(b), the length of puncture polar code is 420, and code rate is 2/3. Compared with WQP algorithm, the proposed algorithms provide gains of about 0.43 dB and 0.55 dB respectively at BER of 10⁻³.

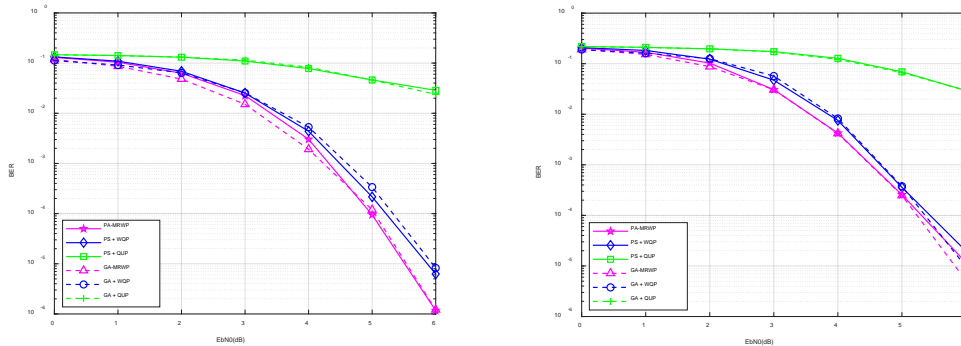


(a) (512, 400, 200) Puncture polar codes

(b) (512, 420, 280) Puncture polar codes

Fig. 6. Performance comparison of different puncture algorithms for different code rate

In Fig. 7, the BER of different puncture algorithms under CA-SCL decoding algorithm is given. The original code length is 256 and list size $L = 8$. After puncture, the code length is 160, and code rate of puncture polar code is 1/2 in Fig. 7(a). The proposed PA-MRWP algorithm and GA-MRWP algorithm can get 0.23 dB and 0.28 dB gain than WQP algorithm respectively at BER of 10⁻⁴. In Fig. 7(b), the length of puncture polar code is 180, and code rate is 2/3. Compared with WQP algorithm, the proposed algorithms provide gains of about 0.13 dB and 0.12 dB respectively at BER of 10⁻⁴.



(a) (256, 160, 80) Puncture polar codes (b) (256, 180, 120) Puncture polar codes
Fig. 7. Performance comparison of different puncture algorithms for different code rate

5. Conclusion

PA-MRWP puncture polar code construction algorithm is proposed in this paper. It is actually a two-step puncture selection strategy, MRWP is used for primary selection and polar spectrum auxiliary puncture is used for adjustment. The MRWP considers the row weight of generator matrix for polar codes, and the rows with the minimum row weight is selected for puncture. If the row with the same rows cannot be punctured all, polar spectrum auxiliary (PA) method is used. Simulation results confirm that proposed PA-MRWP algorithms outperform WQP and QUP algorithms. Moreover, the calculation of both the row weight of the Generator matrix and the polar spectrum proposed in this paper is independent of the real-time signal-to-noise ratio and can be carried out offline.

References

- [1] E. Arıkan, "Channel polarization: A method for constructing capacity-achieving codes," in *Proc. of 2008 IEEE International Symposium on Information Theory*, Toronto, ON, Canada, pp. 1173-1177, 2008. [Article \(CrossRef Link\)](#)
- [2] E. Arıkan, "Channel Polarization: A Method for Constructing Capacity-Achieving Codes for Symmetric Binary-Input Memoryless Channels," *IEEE Transactions on Information Theory*, vol. 55, no. 7, pp. 3051-3073, July 2009. [Article \(CrossRef Link\)](#)
- [3] R. Mori and T. Tanaka, "Performance of Polar Codes with the Construction using Density Evolution," *IEEE Communications Letters*, vol. 13, no. 7, pp. 519-521, July 2009. [Article \(CrossRef Link\)](#)
- [4] P. Trifonov, "Efficient Design and Decoding of Polar Codes," *IEEE Transactions on Communications*, vol. 60, no. 11, pp. 3221-3227, November 2012. [Article \(CrossRef Link\)](#)
- [5] G. He et al., "Beta-Expansion: A Theoretical Framework for Fast and Recursive Construction of Polar Codes," in *Proc. of GLOBECOM 2017 - 2017 IEEE Global Communications Conference*, pp. 1-6, 2017. [Article \(CrossRef Link\)](#)
- [6] A. Eslami and H. Pishro-Nik, "A practical approach to polar codes," in *Proc. of 2011 IEEE International Symposium on Information Theory Proceedings*, pp. 16-20, 2011. [Article \(CrossRef Link\)](#)
- [7] K. Niu, K. Chen and J. Lin, "Beyond turbo codes: Rate-compatible punctured polar codes," in *Proc. of 2013 IEEE International Conference on Communications (ICC)*, pp. 3423-3427, 2013. [Article \(CrossRef Link\)](#)

- [8] R. Wang and R. Liu, "A Novel Puncturing Scheme for Polar Codes," *IEEE Communications Letters*, vol. 18, no. 12, pp. 2081-2084, Dec. 2014. [Article \(CrossRef Link\)](#)
- [9] V. Bioglio, F. Gabry and I. Land, "Low-Complexity Puncturing and Shortening of Polar Codes," in *Proc. of 2017 IEEE Wireless Communications and Networking Conference Workshops (WCNCW)*, pp. 1-6, 2017. [Article \(CrossRef Link\)](#)
- [10] S. Hong and M. Jeong, "An Efficient Construction of Rate-Compatible Punctured Polar (RCPP) Codes Using Hierarchical Puncturing," *IEEE Transactions on Communications*, vol. 66, no. 11, pp. 5041-5052, Nov. 2018. [Article \(CrossRef Link\)](#)
- [11] L. Li, W. Song and K. Niu, "Optimal Puncturing of Polar Codes With a Fixed Information Set," *IEEE Access*, vol. 7, pp. 65965-65972, 2019. [Article \(CrossRef Link\)](#)
- [12] W. Liu, Y. Wang, A. Li, P. Yu and F. Zhou, "An Improved Puncturing Scheme for Polar Codes," in *Proc. of 2020 International Wireless Communications and Mobile Computing (IWCMC)*, pp. 154-158, 2020. [Article \(CrossRef Link\)](#)
- [13] K.Mueadkhunthod, L.Min Min Myint,P. Supnithi,W. Phakphisut. "Construction of Punctured Polar Codes Based on Genetic Algorithm," in *Proc. of 2021 International Conference on Electrical Engineering/Electronics, Computer, Telecommunications and Information Technology (ECTI-CON)*, pp 378-381, 2021. [Article \(CrossRef Link\)](#)
- [14] J. Zhao, W. Zhang and Y. Liu, "A Novel Puncturing Scheme of Low Rate Polar Codes Based on Fixed Information Set," *IEEE Communications Letters*, vol. 25, no. 7, pp. 2104-2108, July 2021. [Article \(CrossRef Link\)](#)
- [15] S. Han, B. Kim, J. Ha, "Rate-Compatible Punctured Polar Codes," *IEEE Communications Letters*, Vol.26, No.4, pp. 753 – 757, April 2022. [Article \(CrossRef Link\)](#)
- [16] M.Vera, V. Branka, Y. Li. "Computing the Partial Weight Distribution of Punctured, Shortened, Precoded Polar Codes" *IEEE Transactions on Communications*, Vol. 70, No.11, pp. 7146 – 7159, November 2022. [Article \(CrossRef Link\)](#)
- [17] K. Niu, Y. Li and W. Wu, "Polar Codes: Analysis and Construction Based on Polar Spectrum," *arXiv preprint arXiv:1908.05889*, 2019. [Article \(CrossRef Link\)](#)
- [18] K. Niu and K. Chen, "CRC-Aided Decoding of Polar Codes," *IEEE Communications Letters*, vol. 16, no. 10, pp. 1668-1671, October 2012. [Article \(CrossRef Link\)](#)



Liu Daofu is a Master student in Hangzhou Dianzi University. He received the B.E. degree in Communication Engineering from Zhengzhou University of Aeronautics, in 2019. His research interests include channel coding and wireless communication.



Guo Rui received the Ph.D. degree from the Zhejiang University, Hangzhou, China, in 2007. He is currently an associate professor with the School of Communication Engineering, Hangzhou Dianzi University, Hangzhou, China. He is a visiting scholar at Oregon State University from August 2018 to August 2019. His research interests include wireless communication and channel coding.